

High-Capacity Methane Storage in Metal–Organic Frameworks $M_2(\text{dhtp})$: The Important Role of Open Metal Sites

Hui Wu,^{†,‡} Wei Zhou,^{*,†,‡} and Taner Yildirim^{†,§}

NIST Center for Neutron Research, National Institute of Standards and Technology, Gaithersburg, Maryland 20899-6102, Department of Materials Science and Engineering, University of Maryland, College Park, Maryland 20742-2115, and Department of Materials Science and Engineering, University of Pennsylvania, Philadelphia, Pennsylvania 19104-6272

Received January 15, 2009; E-mail: wzhou@nist.gov

Abstract: We found that metal–organic framework (MOF) compounds $M_2(\text{dhtp})$ (open metal $M = \text{Mg}, \text{Mn}, \text{Co}, \text{Ni}, \text{Zn}$; $\text{dhtp} = 2,5\text{-dihydroxyterephthalate}$) possess exceptionally large densities of open metal sites. By adsorbing one CH_4 molecule per open metal, these sites alone can generate very large methane storage capacities, $160\text{--}174 \text{ cm}^3(\text{STP})/\text{cm}^3$, approaching the DOE target of $180 \text{ cm}^3(\text{STP})/\text{cm}^3$ for material-based methane storage at room temperature. Our adsorption isotherm measurements at 298 K and 35 bar for the five $M_2(\text{dhtp})$ compounds yield excess methane adsorption capacities ranging from 149 to $190 \text{ cm}^3(\text{STP})/\text{cm}^3$ (derived using their crystal densities), indeed roughly equal to the predicted, maximal adsorption capacities of the open metals (within $\pm 10\%$) in these MOFs. Among the five isostructural MOFs studied, $\text{Ni}_2(\text{dhtp})$ exhibits the highest methane storage capacity, $\sim 200 \text{ cm}^3(\text{STP})/\text{cm}^3$ in terms of absolute adsorption, potentially surpassing the DOE target by $\sim 10\%$. Our neutron diffraction experiments clearly reveal that the primary CH_4 adsorption occurs directly on the open metal sites. Initial first-principles calculations show that the binding energies of CH_4 on the open metal sites are significantly higher than those on typical adsorption sites in classical MOFs, consistent with the measured large heats of methane adsorption for these materials. We attribute the enhancement of the binding strength to the unscreened electrostatic interaction between CH_4 and the coordinatively unsaturated metal ions.

Introduction

Porous metal–organic frameworks (MOFs) are a relatively new family of materials, possessing great potential for many applications, such as gas separation and storage.^{1–3} In particular, studies focused on using MOFs to store energy carrier gases (e.g., hydrogen and methane) have been actively pursued in the past decade.¹ Among the many developments, particularly interesting is a recent report⁴ showing that MOF compound PCN-14 exhibits an absolute methane adsorption capacity of $\sim 230 \text{ cm}^3(\text{STP})/\text{cm}^3$ (standard temperature and pressure equivalent volume of methane per volume of the adsorbent material) at 290 K and 35 bar, a value surpassing that of compressed natural gas storage in current practice and the DOE target⁵ for material-based methane storage [$180 \text{ cm}^3(\text{STP})/\text{cm}^3$ at 298 K and 35 bar].⁶ To our knowledge, PCN-14 is the first and only MOF reported so far to join the rare group of materials known

to potentially meet the DOE target.^{4,7,8} The excellent adsorption capacity and large isosteric heat of adsorption (Q_{st}) of CH_4 ($\sim 30 \text{ kJ/mol}$) found in PCN-14 were attributed to several of its structural features, including (a) the aromatic rings on the organic linker, which are presumably good for methane binding, and (b) the size and geometry of the nanopores, which appear to be just “right” for enabling multiple interactions between the CH_4 molecule and the host framework.⁴ Additionally, we note that PCN-14 contains coordinatively unsaturated Cu ions, which may also significantly contribute to its impressive methane adsorption behavior. Clearly, a full understanding of all these

- (6) It is important to note that almost all reported values for the methane adsorption capacities in MOF materials are based on the ideal densities of MOF crystals. In practice, MOF materials are usually in microcrystalline powder forms. When the “packing factor” of the powders is taken into account, the actual volumetric adsorption capacities would be less than the reported, ideal values. Therefore, there are still strong driving forces for discovering new MOF materials with even higher ideal adsorption capacities than that reported for PCN-14.
- (7) (a) Menon, V. C.; Komarneni, S. *J. Porous Mater.* **1998**, *5*, 43. (b) Noro, S.-i.; Kitagawa, S.; Kondo, M.; Seki, K. *Angew. Chem., Int. Ed.* **2000**, *39*, 1433. (c) Kondo, M.; Shimamura, M.; Noro, S.-i.; Minakoshi, S.; Asami, A.; Seki, K.; Kitagawa, S. *Chem. Mater.* **2000**, *12*, 1288. (d) Eddaoudi; Kim, J.; Rosi, N.; Vodak, D.; Wachter, J.; O’Keeffe, M.; Yaghi, O. M. *Science* **2002**, *295*, 469. (e) Düren, T.; Sarkisov, L.; Yaghi, O. M.; Snurr, R. Q. *Langmuir* **2004**, *20*, 2683. (f) Bourrelly, S.; Llewellyn, P. L.; Serre, C.; Millange, F.; Loiseau, T.; Férey, G. *J. Am. Chem. Soc.* **2005**, *127*, 13519.
- (8) Wang, X.-S.; Ma, S.; Rauch, K.; Simmons, J. M.; Yuan, D.; Wang, X.-S.; Yildirim, T.; Cole, W. C.; Lopez, J. J.; De Meijere, A.; Zhou, H.-C. *Chem. Mater.* **2008**, *20*, 3145.

[†] National Institute of Standards and Technology.

[‡] University of Maryland.

[§] University of Pennsylvania.

- (1) (a) Ockwig, N.; Friedrichs, O. D.; O’Keeffe, M.; Yaghi, O. M. *Acc. Chem. Res.* **2005**, *38*, 176. (b) Férey, G. *Chem. Soc. Rev.* **2008**, *37*, 191. (c) Morris, R. E.; Wheatley, P. S. *Angew. Chem., Int. Ed.* **2008**, *47*, 4966. (d) Zhao, D.; Yuan, D.; Zhou, H.-C. *Energy Environ. Sci.* **2008**, *1*, 222.
- (2) Rowsell, J. L. C.; Yaghi, O. *Angew. Chem., Int. Ed.* **2005**, *44*, 4670–4679.
- (3) Dinca, M.; Long, J. R. *Angew. Chem., Int. Ed.* **2008**, *47*, 6766–6779.
- (4) Ma, S.; Sun, D.; Simmons, J. M.; Collier, C. D.; Yuan, D.; Zhou, H.-C. *J. Am. Chem. Soc.* **2008**, *130*, 1012–1016.
- (5) Burchell, T.; Rogers, M. *SAE Tech. Pap. Ser.* **2000**, 2001–2205.

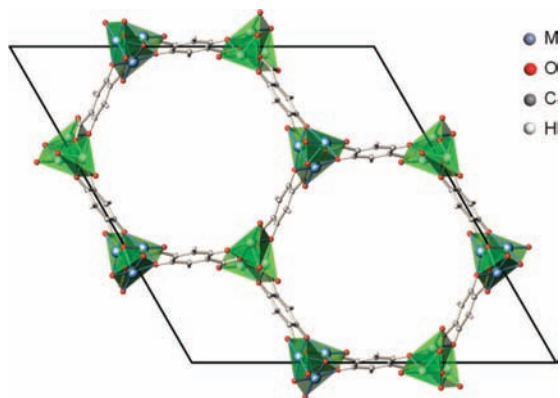


Figure 1. Crystal structure of $M_2(\text{dhtp})$, [001] view. The one-dimensional (1-D) channel pore geometry is apparent. The open metal ions, bonded with five oxygen atoms in a square-pyramid coordination environment, are highlighted for clarity.

interplaying factors is necessary for further, rational development of new MOF materials with even higher methane storage capacities.

In this work, we focused on elucidating the role of open metal sites on the adsorption of methane. The open metal sites are well-known to exhibit enhanced binding strength for H_2 gas,³ mainly due to the unscreened Coulomb interaction between the metal ion and H_2 .⁹ Although the CH_4 molecule is highly symmetric and nonpolar, some enhancement of binding strength is still possible, since adsorption on the metal site would perturb the charge distribution of the CH_4 molecule, reduce the molecular symmetry, and induce multipole moments. We note that, in PCN-14, if all of the open Cu sites are saturated by binding one methane molecule per Cu ion, it would give an adsorption capacity of $\sim 59 \text{ cm}^3(\text{STP})/\text{cm}^3$, roughly one-quarter of the total capacity as measured at 290 K and 35 bar. In searching for other MOFs with open metals that may also possess high methane storage capacity, we noticed that the recently reported^{10–12} isostructural $M_2(\text{dhtp})$ [M: open metal, $\text{dhtp} = 2,5\text{-dihydroxyterephthalate}$; chemical formula: $M_2(\text{C}_8\text{H}_2\text{O}_6)$] MOF series (see Figure 1) have significantly higher densities of open metal sites in their crystal structures ($\sim 4.5 \text{ sites}/\text{nm}^3$) than PCN-14 ($\sim 1.6 \text{ sites}/\text{nm}^3$). If the binding strength of CH_4 on the open metal sites in $M_2(\text{dhtp})$ is large enough for room-temperature adsorption, saturating these metal sites could provide an exceptionally high adsorption capacity, ranging from 160 to 174 $\text{cm}^3(\text{STP})/\text{cm}^3$ (see Table 1). Furthermore, with a little help from possible additional adsorption sites in these MOF structures, the material performance could easily surpass the DOE target [$180 \text{ cm}^3(\text{STP})/\text{cm}^3$].

(9) Zhou, W.; Yildirim, T. *J. Phys. Chem. C* **2008**, *112*, 8132–8135.

(10) (a) Rosi, N. L.; Kim, J.; Eddaoudi, M.; Chen, B. L.; O’Keeffe, M.; Yaghi, O. M. *J. Am. Chem. Soc.* **2005**, *127*, 1504. (b) Dietzel, P. D. C.; Morita, Y.; Blom, R.; Fjellvag, H. *Angew. Chem., Int. Ed.* **2005**, *44*, 6354. (c) Dietzel, P. D. C.; Panella, B.; Hirscher, M.; Blom, R.; Fjellvag, H. *Chem. Commun.* **2006**, 959. (d) Dietzel, P. D. C.; Blom, R.; Fjellvag, H. *Eur. J. Inorg. Chem.* **2008**, 3624–3632. (e) Caskey, S. R.; Wong-Foy, A. G.; Matzger, A. J. *J. Am. Chem. Soc.* **2008**, *130*, 10870–10871.

(11) Zhou, W.; Wu, H.; Yildirim, T. *J. Am. Chem. Soc.* **2008**, *130*, 15268–15269.

(12) Note that, in the literature, $\text{Zn}_2(\text{dhtp})$ was also called MOF-74, while some other $M_2(\text{dhtp})$ ’s were named CPO-27-M. Also note that although “dhtp” is widely used in the literature to represent the organic linker in this series of MOF compounds, a more appropriate name might be “2,5-dioxido-1,4-benzene-dicarboxylate (DOBDC)”, as suggested recently in ref 10e. For historic reasons, here we continue to use the well-known “dhtp” representation.

Table 1. Summary of Data Obtained for $M_2(\text{dhtp})$ ^{a,b}

MOF compound	open M	ρ (g/cm ³)	max CH_4 ads on open M [$\text{cm}^3(\text{STP})/\text{cm}^3$]	exp CH_4 ads [$\text{cm}^3(\text{STP})/\text{cm}^3$]	initial Q_{st} (kJ/mol)	$d(\text{M}-\text{C})$ (Å)	E_{B} (kJ/mol)
$\text{Mg}_2(\text{dhtp})$	Mg	0.909	168	149	18.5	2.64	33.8
$\text{Mn}_2(\text{dhtp})$	Mn	1.084	160	158	19.1	2.73	29.8
$\text{Co}_2(\text{dhtp})$	Co	1.169	168	174	19.6	2.74	29.7
$\text{Ni}_2(\text{dhtp})$	Ni	1.206	174	190	20.2	2.58	34.8
$\text{Zn}_2(\text{dhtp})$	Zn	1.231	170	171	18.3	2.72	29.7
PCN-14	Cu	0.871	59	220	30.0	/	/
PCN-11	Cu	0.749	70	170	14.6	2.62	24.7
MOF-5 ^c	(Zn)	0.593	(69)	110	12.2	(3.69)	(20.7)

^a Data include the open metal species, crystal density (ρ), the ideal saturated CH_4 adsorption capacity on open metals (max CH_4 ads on open M), experimental excess CH_4 adsorption capacity at 298 K, 35 bar (exp CH_4 ads), the experimental initial isosteric heat of adsorption (Q_{st}) for CH_4 , the calculated metal–C distance (d , from LDA), and the calculated static binding energy of CH_4 on the open metal (E_{B} , also from LDA). ^b Available experimental data for PCN-14, PCN-11, and MOF-5 (adopted from refs 4, 8, and 14, respectively) are also shown in the table for comparison purposes. ^c The metal ion in MOF-5 is fully coordinated (not open metal), thus the corresponding values are shown in parentheses.

Motivated by these observations, we performed a systematic methane adsorption study on the $M_2(\text{dhtp})$ (M = Mg, Mn, Co, Ni, Zn) series of MOF compounds. Our adsorption isotherm measurements confirmed that these materials indeed exhibit a high methane excess adsorption capacity. Neutron diffraction experiments clearly revealed the primary CH_4 binding sites being the open metals. The measured isosteric heats of adsorption are significantly higher than those found in classical MOFs without open metal sites. The enhanced CH_4 binding strength on the open metal is further confirmed by our initial first-principles calculations.

Experimental Section

The five $M_2(\text{dhtp})$ (M = Mg, Mn, Co, Ni, Zn) samples used in this work were synthesized and fully activated as described in detail in one of our recent publications.¹¹ Briefly, the synthesis process is based on a literature protocol of a solvothermal reaction between M^{2+} salt and 2,5-dihydroxyterephthalic acid dissolved in a solvent mainly containing dimethylformamide (DMF), first reported by Rosi et al. and Dietzel et al.¹⁰ The sample activation occurred at elevated temperature (473 K) in a dynamic vacuum for 3 days. All activated samples were confirmed to possess high crystallinity and to contain no leftover solvent molecules by element analysis using the neutron prompt- γ activation analysis¹³ (PGAA).

Methane adsorption and desorption isotherms (at 270, 280, and 298 K) were measured on the five fully activated $M_2(\text{dhtp})$ samples using a Sieverts-type apparatus. The adsorption isotherms were then used to derive the heats of CH_4 adsorption, using the modified Clausius–Clapeyron equation. A detailed description of our experimental setup, calibration, and the isotherm and Q_{st} data analysis can also be found in a previous publication.¹⁴

Neutron powder diffraction measurements were performed on a bare $\text{Mg}_2(\text{dhtp})$ sample, and the same sample loaded with various amounts of CD_4 . Deuterated methane was used here for the purpose of obtaining higher-quality diffraction spectra, by avoiding the large incoherent neutron scattering cross section of H presented in CH_4 . Data were collected on the High Resolution Neutron Powder Diffractometer (BT-

(13) Lindstrom, R. M. *J. Res. Natl. Inst. Stand. Technol.* **1993**, *98*, 127–133.

(14) Zhou, W.; Wu, H.; Hartman, M. R.; Yildirim, T. *J. Phys. Chem. C* **2007**, *111*, 16131–16137.

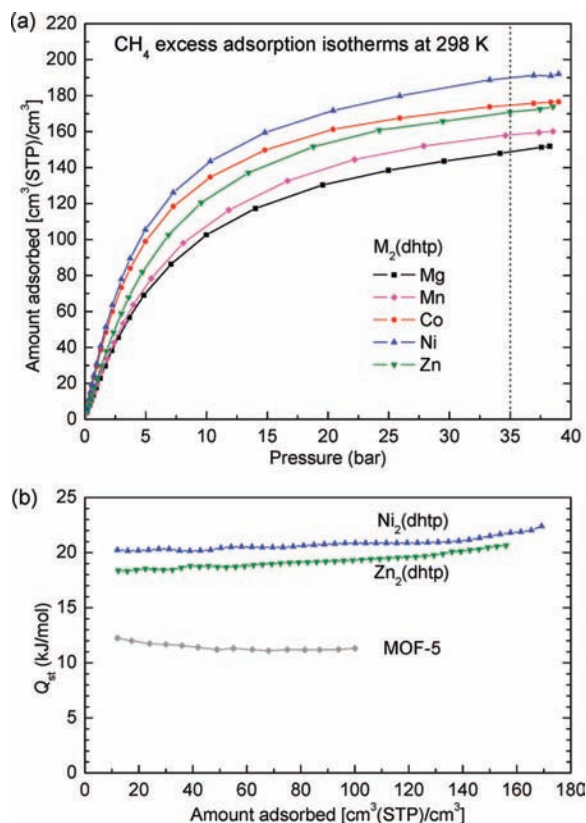


Figure 2. (a) Excess CH₄ adsorption isotherms of M₂(dhtp) at 298 K. (b) The experimental Q_{st} of Ni₂(dhtp) and Zn₂(dhtp) (the error bar is $\sim \pm 5\%$). The Q_{st} 's of Mg₂(dhtp), Mn₂(dhtp), and Co₂(dhtp) fall between the two curves and, thus, are not shown for clarity. The Q_{st} 's of MOF-5 (from ref 14) are also plotted for comparison.

1) at the NIST Center for Neutron Research. Rietveld structural refinements were done using the GSAS package.¹⁵

First-principles calculations based on density-functional theory (DFT) were performed using the PWSCF package.¹⁶ We used Vanderbilt-type ultrasoft pseudopotentials and tested both the generalized gradient approximation (GGA) with the Perdew–Burke–Ernzerhof exchange correlation and the local-density approximation (LDA) with the Perdew–Zunger exchange correlation. A cutoff energy of 544 eV and a $2 \times 2 \times 2$ k -point mesh were found to be sufficient for the total energy to converge within 0.5 meV/atom. We first optimized the primitive cell of the M₂(dhtp) structure, which contains 54 atoms. To obtain the CH₄ binding energy on open metal sites, six CH₄ molecules were introduced to the optimized M₂(dhtp) structure (guided by the diffraction results), followed by a structural relaxation. As a reference, a CH₄ molecule placed in a supercell with the same cell dimensions was also relaxed. The static binding energy was then calculated using $E_B = E[M_2(dhtp)] + 6E(CH_4) - E[M_2(dhtp) + 6CH_4]$.

Results and Discussion

The excess CH₄ adsorption isotherm curves at 298 K are shown in Figure 2a for the five M₂(dhtp) samples. Note that the adsorption and desorption isotherm curves overlap with each other with no hysteresis observed (for clarity, the desorption isotherm curves are not shown in the figure). Full reversibility

and fast kinetics are expected, since the host M₂(dhtp) MOF structures have relatively large (~ 13.6 Å) one-dimensional channel pores (see Figure 1), which can be easily accessed by a methane gas molecule (with a kinetic diameter of ~ 3.8 Å).

The excess adsorption capacities of CH₄ in M₂(dhtp) MOFs at 298 K and 35 bar range from 149 to 190 cm³(STP)/cm³. Note that these volumetric values were converted from the directly measured gravimetric capacities using the MOF crystal densities (same method was used previously^{4,7,8} for other MOFs, including PCN-14), thus representing the ideal maximal methane storage capacities that these MOF materials can generate in practice.¹⁷ Among the various MOFs, Ni₂(dhtp) exhibits the highest excess adsorption capacity. In terms of absolute methane adsorption,¹⁸ the value is slightly higher, ~ 200 cm³(STP)/cm³ for Ni₂(dhtp), potentially surpassing the DOE target [180 cm³(STP)/cm³] by $\sim 10\%$.

To derive the isosteric heat of adsorption, isotherm data at two lower temperatures (280 and 270 K) were also collected [see Figure S1 in the Supporting Information (SI)]. Figure 2b shows the heats of adsorption as a function of CH₄ loading for Ni₂(dhtp) and Zn₂(dhtp). The Q_{st} values for the other three compounds fall between these two curves and, thus, are not plotted for clarity. Overall, all five M₂(dhtp) compounds exhibit very similar heats of adsorption in the range ~ 18.3 – 20.2 kJ/mol at low CH₄ loading (also see Table 1), which are significantly larger than those of classical MOFs with fully coordinated metal sites. For comparison, the Q_{st} 's of metal–organic framework-5 (MOF-5, the most widely studied MOF compound) from the literature¹⁴ are also shown in Figure 2b. The initial Q_{st} of M₂(dhtp) is $\sim 50\%$ higher than that of MOF-5 (~ 12.2 kJ/mol). Within the M₂(dhtp) series, Ni₂(dhtp) has the highest Q_{st} (despite the small difference), consistent with the fact that it adsorbs the largest amount of CH₄ per unit volume.

To fully understand the high methane uptake and large Q_{st} observed in these MOFs, structural information of the adsorbed CH₄ is essential. Of the five M₂(dhtp) compounds, we picked Mg₂(dhtp) for a detailed diffraction study. We assume that if the primary adsorption of CH₄ in Mg₂(dhtp) occurs on the open metals, the same has to be true for other M₂(dhtp) members, since they are isostructural and Mg₂(dhtp) has one of the lowest, initial Q_{st} values (18.5 kJ/mol) within the series.

The observed and refined neutron diffraction profiles of the bare Mg₂(dhtp) sample, and the same sample with two different methane loadings (0.73 and 1.23 CD₄/Mg) are shown in Figure

(17) Only for a single-crystal bulk sample, such an ideal adsorption capacity becomes the real storage capacity. So far we have not been able to grow single crystals large enough for isotherm measurements. The assembly of microcrystalline MOF powders into a bulk material is an engineering issue. Our preliminary effort on packing MOF powders into a bulk pellet sample under hydrostatic pressure shows that a packing density of 80–85% can be easily achieved without collapsing the MOF crystal. This packing density might be further improved in the future but would certainly still be less than that of a single crystal. Here we focus on the ideal volumetric capacities derived using the MOF crystal densities, to compare the intrinsic properties of different MOFs.

(18) Note that the absolute adsorption is the total amount of gas introduced to the sample cell minus the amount outside the sample in the gas phase; thus, it accounts for the total amount of adsorbate molecules residing in pores. The excess adsorption is the absolute amount of gas contained in the sample pores less the amount of gas that would be present in the pores in the absence of gas–solid intermolecular forces. Excess adsorption capacity is a “material property”; thus it is what is usually reported in the literature and can be used to compare different materials. When one compares the performance of “materials-based gas storage” with “compressed gas storage”, “absolute adsorption capacity” is the more proper one to use.

(15) Larson, A. C.; Von Dreele, R. B. General Structure Analysis System, Report LAUR 86-748. Los Alamos National Laboratory, NM, 1994.

(16) Baroni, S.; Dal Corso, A.; de Gironcoli, S.; Giannozzi, P.; Cavazzoni, C.; Ballabio, G.; Scandolo, S.; Chiarotti, G.; Focher, P.; Pasquarello, A.; Laasonen, K.; Trave, A.; Car, R.; Marzari, N.; Kokalj, A. Quantum-ESPRESSO; <http://www.pwscf.org/>.

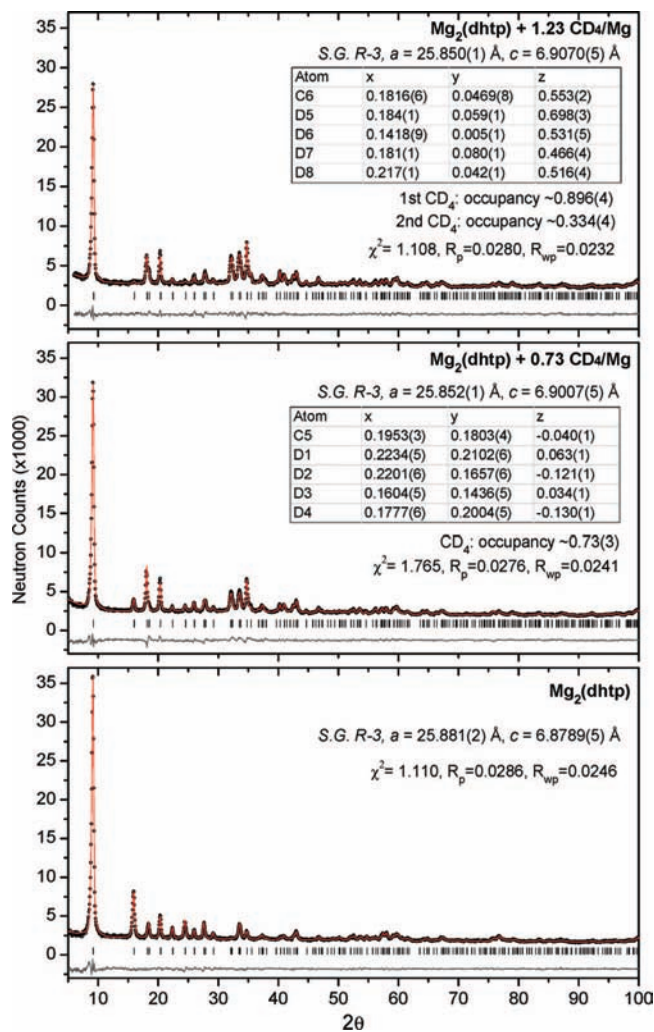


Figure 3. Observed (dots), refined (line), and difference (noisy line) neutron powder diffraction profiles for bare Mg₂(dhtp) and Mg₂(dhtp) with CD₄ loadings of 0.73 and 1.23 CD₄/Mg. The coordinates of the adsorbed CD₄ (sites I and II) are shown in the inset tables.

3. Using the Fourier difference technique,^{19,20} we were able to unambiguously identify the location and orientation of the adsorbed methane molecules, which we followed with a full-profile Rietveld refinement. The refined CH₄ coordinates are given in the inset tables of Figure 3, while detailed information of the whole crystal structure can be found in the SI. For the 0.73 CD₄/Mg loading, all methane molecules go to site I, while, for the 1.23 CD₄/Mg loading, site I is roughly 90% populated while site II has an occupancy of ~33%.

The geometries of the adsorbed methane molecules (sites I and II) with respect to the Mg₂(dhtp) host structure are shown in Figure 4. As expected, the primary gas adsorption in M₂(dhtp) indeed occurs directly on the open metal sites (site I), similar to previous observations for other gas molecules [H₂ in Zn₂(dhtp), and CO₂ and NO in Ni₂(dhtp)].^{21–23} The CH₄

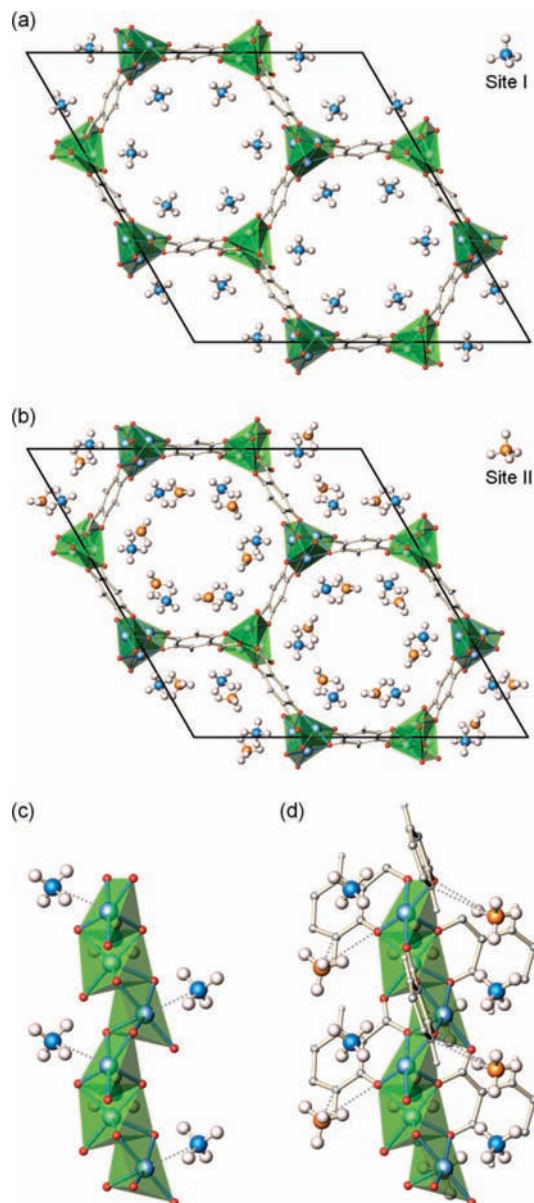


Figure 4. (a) Crystal unit cell of Mg₂(dhtp) with methane adsorbed on site I (the open metal site), as determined from neutron diffraction. Note that each metal ion directly binds to one methane molecule. (b) Experimental Mg₂(dhtp) structure with methane adsorbed on both sites I and II. (c) A close view of methane location and orientation with respect to the metal–oxide pyramids and the organic linkers.

molecule assumes an orientation such that it “sits” on the square plane of the MgO₅ pyramid, to maximize its interaction with the metal cluster. The experimental Mg–C distance is 3.04 Å, a fairly small value (e.g., compared to the experimental C–C distance of CH₄ adsorbed on graphite surface, 3.45 Å²⁴), which implies a relatively strong interaction between methane molecules and the coordinatively unsaturated Mg atoms. Also note that the distance of two nearest-neighbor CH₄ molecules is 4.90 Å, much larger than that in solid methane (~3.96 Å), suggesting that the interference between adsorbed methane molecules is rather weak when only the first sites are occupied. This explains

(19) (a) Yildirim, T.; Hartman, M. R. *Phys. Rev. Lett.* **2005**, *95*, 215504.
 (b) Wu, H.; Zhou, W.; Yildirim, T. *J. Am. Chem. Soc.* **2007**, *129*, 5314.

(20) Wu, H.; Zhou, W.; Yildirim, T. *J. Phys. Chem. C* **2009**, *113*, 3029.

(21) Liu, Y.; Kabbour, H.; Brown, C. M.; Neumann, D. A.; Ahn, C. C. *Langmuir* **2008**, *24*, 4772.

(22) McKinlay, A. C.; Xiao, B.; Wragg, D. S.; Wheatley, P. S.; Megson, I. L.; Morris, R. E. *J. Am. Chem. Soc.* **2008**, *130*, 10440–10444.

(23) Dietzel, P. D. C.; Johnsen, R. E.; Fjellvag, H.; Bordiga, S.; Groppo, E.; Chavan, S.; Blom, R. *Chem. Commun.* **2008**, 5125.

(24) Vidali, G.; Ihm, G.; Kim, H.-Y.; Cole, M. W. *Surf. Sci. Rep.* **1991**, *12*, 133.

well why the observed Q_{st} curves are relatively “flat” from low loading up to a point where most of the first sites are occupied.

The second methane site is an “add-on” adsorption site (i.e., this site only exists after the first site is occupied). The neighboring methane molecules on sites I and II have a distance of ~ 3.73 Å, slightly smaller than that in solid methane, suggesting that the adsorbed CH₄ molecule on site II is stabilized through its interactions with both the framework (mainly the C, O atoms on the organic linker) and the CH₄ molecules on site I. It also implies that it is possible to achieve high-density methane packing through adsorption.

Using this detailed structural information from neutron diffraction studies, we were able to perform some initial first-principles total energy calculations to help understand the enhanced interaction between the open metals and the methane molecule. We note that the weak dispersive interactions are not properly treated in standard DFT, and thus our goal is limited to gaining some qualitative insight. Calculations using the generalized gradient approximation of DFT predict very weak binding between the open metal and the methane molecule, which clearly indicates that the observed adsorption of methane on the open metal site is not chemisorption (which are well described in GGA) but still mainly physisorption. Therefore, here we focus on results obtained from the local density approximation, which is known to give overestimated binding for weak interactions.

The DFT-LDA optimized structure of Mg₂(dhtp) and the structure with adsorbed methane agree fairly well with the experimental data (see SI). The calculated metal–C distances and binding strengths are summarized in Table 1, along with other experimental data. For the five M₂(dhtp) compounds, the calculated binding energies are quite close, all around 30 kJ/mol, which is in good qualitative agreement with the similar Q_{st} values obtained experimentally. Note that the calculated E_B is the static binding energy at 0 K. We did not correct it for the zero-point motion and the temperature effect, since a quantitative comparison between the experimental Q_{st} and the E_B derived at the current level of DFT is not possible anyway. Also note that the calculated static E_B values are higher than the experimental Q_{st} 's and the calculated Mg–C distance is smaller than the experimental value. This is expected for LDA, which typically overestimates the binding.

In Table 1, for comparison purposes, we also listed the available experimental results from the literature^{4,8,14} for PCN-14, PCN-11, and MOF-5, along with their CH₄ binding energies calculated in this work. PCN-14 and PCN-11 are two MOFs that have the highest methane uptake reported thus far.^{4,7,8} Both of them have the same dimetal paddlewheel-like Cu₂(CO₂)₄ clusters with open Cu sites. The metal–ligand cluster in MOF-5 is OZn₄(CO₂)₆, where Zn is fully coordinated with four O atoms, forming a tetrahedron. Partial structures of DFT-optimized PCN-11 and MOF-5 with adsorbed methane are shown in Figure 5. The calculated CH₄ binding energy on the open Cu site in PCN-11 is 24.7 kJ/mol, significantly smaller than those of M₂(dhtp) (~ 30 kJ/mol). This is consistent with the relatively low experimental initial Q_{st} of PCN-11 (14.6 kJ/mol) compared to those of M₂(dhtp) (>18 kJ/mol). For PCN-14, since the open Cu site in its structure is essentially the same as that in PCN-11, the reported, exceedingly high initial Q_{st} (30 kJ/mol) implies that there exist some stronger CH₄ binding sites in this MOF structure other than the open Cu sites. For MOF-5, the calculated methane binding at the cup site (the primary binding site found experimentally²⁰) is only 20.7 kJ/mol, the lowest among all

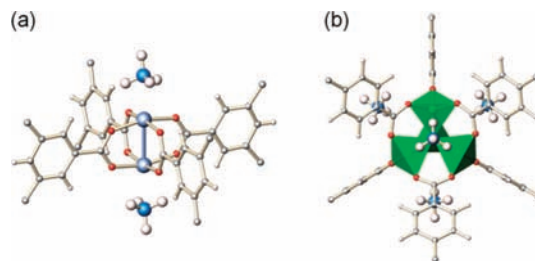


Figure 5. (a) Partial structure of the DFT-optimized PCN-11 crystal with CH₄ molecules adsorbed on the open Cu metal sites. (b) Partial structure of the DFT-optimized MOF-5 crystal with CH₄ molecules adsorbed on the “cup” sites of the OZn₄(CO₂)₆ cluster.

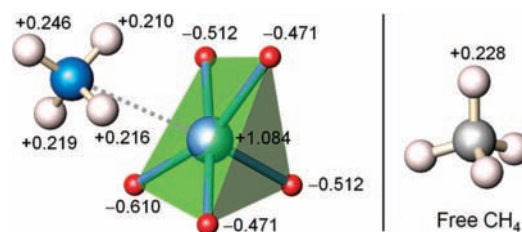


Figure 6. Projected Löwdin charges of the methane molecule adsorbed on the open Mg site in Mg₂(dhtp) MOF. The adsorbed CH₄ is slightly distorted with an uneven charge distribution, which enhances the electrostatic interaction with the open metal charges. For comparison, the Löwdin charge of the H atom in a free CH₄ gas molecule is also shown.

MOFs investigated, which is again consistent with its experimental Q_{st} being the lowest.

Overall, the energies derived from DFT calculations are in qualitative agreement with experimental heats of adsorption. Both clearly show that the methane affinities on the open metals are enhanced compared to nonopen metals. We believe that the origin of the enhancement is due to the unscreened electrostatic interaction between CH₄ and the coordinatively unsaturated metal ion, similar to what we found previously for H₂ adsorption on open metals.^{9,11} In Figure 6, we show the projected atomic charges of the methane molecule adsorbed on the open Mg site in Mg₂(dhtp), from a Löwdin population analysis.²⁵ Unlike the highly symmetric, free CH₄ molecule, the adsorbed CH₄ is slightly distorted with a perturbed charge distribution. As a consequence, there exists an enhanced Coulomb interaction between the distorted CH₄ molecule and the open metal charge density.

When different open metals were compared, Cu appeared to have a weaker CH₄ binding enhancement (this may be due in part to the paddlewheel-like geometry of the Cu₂(CO₂)₄ clusters), while the other five (Mg, Mn, Co, Ni, and Zn) are quite similar (although both calculation and experimental data suggest that Ni is slightly stronger than others). Overall, the dependence of the CH₄ binding strength compared to that of H₂ on different metals is much weaker.¹¹ This is likely because of the larger size of the CH₄ molecule. For a metal ion with a small radius (such as Ni), the H₂ molecule can bind very closely (~ 2.0 Å) to the open metal, resulting in significant charge overlap and thus a large enhancement of the binding strength.¹¹ Depending on the metal ion radius, the M–H₂ distance varies widely from ~ 2.0 Å (Ni) to ~ 2.8 Å (Zn).¹¹ In the case of methane, the M–C distance is largely constrained by the CH₄ geometry (a steric effect) and thus varies very little among different metals. This

(25) Löwdin, P. O. *Adv. Quantum Chem.* **1970**, *5*, 185.

makes the CH₄ binding strength nearly independent of the open metal species.

Next, we discuss how the number of open metal sites relates to the adsorption capacity. For M₂(dhtp), the excess CH₄ adsorption capacity at 298 K and 35 bar is roughly equal to the saturating adsorption capacity on the open metal site, within $\pm 10\%$. This clearly shows that open metal sites are primarily responsible for the high methane uptake in these materials under ambient conditions. In contrast, in PCN-11 and PCN-14, the open metal capacity is only a small fraction of the total adsorption, meaning that there are a large number of other strong adsorption sites available. Future investigations are highly desired to elucidate the location and nature of these other important adsorption sites.

All the above results on M₂(dhtp) clearly demonstrate the important role that open metal sites can play in MOFs to achieve high-capacity methane adsorption at room temperature and moderate pressure. One disadvantage of these open metal sites is also obvious: metal elements are heavy, and each metal can only bind to one methane molecule in the current five-coordination case. Indeed, the crystal density of all these M₂(dhtp) compounds are higher than that of PCN-14, PCN-11, and MOF-5 (see Table 1), making them less attractive in terms of weight capacity. Nevertheless, there is still considerable room to further improve these materials. For M₂(dhtp) compounds, since the current organic linker does not contribute significantly to the room-temperature capacity, further improvement should focus on substituting other organic linkers, particularly those with functional groups that are known to bind CH₄ more favorably. If a strong adsorption site can be generated on the organic linker, or the binding strength of the current secondary adsorption site can be enhanced, the already high methane uptake of M₂(dhtp) can be further increased, which could offset some of the disadvantages of their large mass densities. For PCN-14 and PCN-11, it is worth pursuing the synthesis of MOF

analogues with other open metals, which will likely bind CH₄ stronger than Cu and, thus, improve the overall methane storage capacity.

Conclusions

In summary, we have shown that M₂(dhtp) MOF compounds possess exceptionally large densities of open metal sites. Diffraction experiments confirm that these metal sites are totally responsible for their high-capacity methane adsorption. Among the five isostructural MOFs, Ni₂(dhtp) exhibits the highest absolute adsorption capacity, ~ 200 cm³(STP)/cm³, making it the second MOF material known (to our knowledge) to potentially surpass the DOE target. Experimental heats of adsorption and first-principles calculated binding energies both show that the methane affinity to the open metal ions is significantly stronger than that on typical adsorption sites in classical MOFs. Among various open metals, Ni appears to be slightly better than others, while the overall variation of binding strength with metal species is small. These results provide useful guidance for further improvements on the design of MOFs for methane storage.

Acknowledgment. The authors thank Dr. Jason Simmons for helpful discussions. This work was partially supported by DOE through BES Grant No. DE-FG02-08ER46522 (T.Y.).

Supporting Information Available: N₂ Brunauer–Emmett–Teller (BET) surface areas and pore volumes of our M₂(dhtp) samples. Methane adsorption isotherms of M₂(dhtp) at 280 and 270 K. Crystallographic details on the structures and CD₄ locations of Mg₂(dhtp) with various CD₄ loadings. Atomic coordinates of the DFT-optimized Mg₂(dhtp) structure with adsorbed methane. These materials are available free of charge via the Internet at <http://pubs.acs.org>.

JA900258T